We are IntechOpen, the world's leading publisher of Open Access books Built by scientists, for scientists

6,900
Open access books available

186,000
International authors and editors

200M
Downloads

Our authors are among the

154
Countries delivered to

TOP 1%
most cited scientists

12.2%
Contributors from top 500 universities

WEB OF SCIENCE™

Selection of our books indexed in the Book Citation Index in Web of Science™ Core Collection (BKCI)

Interested in publishing with us?
Contact book.department@intechopen.com

Numbers displayed above are based on latest data collected.
For more information visit www.intechopen.com

Chapter 2

Preparation and Structural Characterization of Metallophthalocyanine Particles Embedded in a Polymer Matrix

María Elena Sánchez-Vergara,
Angelina Romo Ubeda, Enrique Garibay Ochoa and
José Ramón Alvarez-Bada

Additional information is available at the end of the chapter

http://dx.doi.org/10.5772/67576

Abstract

In this work, thin-film deposition of FePc particles nucleated and grown in gels was carried out in air by spin coating. The surface morphology and structure of these films were analysed by scanning electron microscopy (SEM) and Fourier transform infrared (FTIR) spectroscopy. The optical parameters have been investigated using spectrophotometric measurements of transmittance in the wavelength range of 200–1100 nm. The absorption spectra recorded in the UV-Vis region for the deposited samples showed a single band, namely the B or Soret band in the region between 285 and 305 nm. The dependence of the Tauc and Cody optical gaps associated with the thickness of the film was determined and found to be around 4.2 eV from direct transitions and 3.8 eV from non-direct transitions. The films' electric properties and their dependence in the presence of radiation of several wavelengths were evaluated. At lower voltages, ohmic conduction is evident, while space-charge limited conductivity (SCLC) governed by an exponential trap distribution is to be found at higher voltages.

Keywords: thin films, spin coating, metallophthalocyanines, optical properties, electrical properties

1. Introduction

Photoconducting agents and other photoelectronic compounds embedded in polymer films as nanocomposite films have attracted considerable attention, as they exhibit many useful

INTECH
open science | open minds

© 2017 The Author(s). Licensee InTech. This chapter is distributed under the terms of the Creative Commons Attribution License (http://creativecommons.org/licenses/by/3.0), which permits unrestricted use, distribution, and reproduction in any medium, provided the original work is properly cited. CC BY

optical and electrical properties. Because of their large chemical and structural stability, as well as their optical and electrical properties, metallic phthalocyanines (MPcs) have been introduced into polymeric matrices as nanoparticles. A polymeric matrix composite (PMC) is a compound material consisting of a polymeric primary phase, or matrix, which is embedded in a secondary phase based mainly on matrix-reinforcing fibres and particles. The polymeric matrix enhances material stability, as it limits the introduction of environmental oxygen or water, which could reduce the potential usefulness of the MPcs. Nanostructuring also permits two other goals: to achieve optical homogeneity of the polymeric composite medium and to take advantage of specific properties of MPcs in their crystalline form. MPcs are usually ordered in crystalline arrangements, as their aromatic rings stack neatly. Due to the strength of π bonds, MPcs can be accommodated in a large number of different structures, which depend on the substituents they have. The type of structure determines the physical properties of a specific MPc, as well as its applications. The main modes of MPc molecular organization that may be observed are: (i) crystals, which can be in the alpha or beta allotropic forms (the beta polymorph being thermodynamically more stable). The two types are distinguished by the angle formed between the symmetry axis and the stacking direction. Alpha and beta crystals form angles of 26.5 and 45.8°, respectively. (ii) Liquid crystals, where Pcs are substituted by flexible lipophilic chains, which allow the formation by substituents of a quasi-liquid medium surrounding the in-plane aromatic nuclei, which overlap in columns distributed over two-dimensional positions with hexagonal or tetragonal symmetries. (iii) Thin films are solid structures whose thicknesses can be neglected for many physical purposes. In applications involving interaction with electromagnetic waves, thin-film thickness must be of the same order as the wavelength of the interacting disturbance. Thin films represent the Pcs arrangement most commonly considered for electronic applications. (iv) Skewer-structured polymers are obtained by polymerizing MPcs through bridge ligands; due to the variety of ligands that may be used and their properties, the distance between molecules can be controlled rather well and, thanks to the rigidity of the unidirectional connection in this type of structures, very good electronic and optical properties can be obtained from the material.

The purpose of this work is to report the generation of MPc crystals, their dispersion into a polymeric matrix and the evaluation of their optical and electrical properties in thin-film form. In this study, a polystyrene polymeric matrix was used. The materials thus obtained were characterized by different methods, including infrared (IR) and ultraviolet-visible (UV-Vis) spectroscopy, as well as scanning electron microscopy (SEM). First nanoparticles were synthesized in a molecular solution obtained from a supersaturated MPc solution. Second a solid composite was prepared by introducing pre-grown colloidal MPc particles into a polymeric matrix in a spin coating process. Spin coating leads to the production of uniform, flat, high-quality films or coatings. This process involves the application of a certain amount of nanoparticles suspended in a polymer and previously solved in an organic solvent. A small amount of the fluid is put on a substrate attached to a plate that is made to rotate at high speed, so that the resulting centripetal force spreads the suspension until the desired film thickness is achieved for the composite material. This process has four stages: deposition, centrifugation, de-centrifugation and evaporation. The evaporation of the fourth stage represents the main thinning mechanism for the film. After the film is deposited, it is annealed for 10 min at 90°C to accelerate matrix polymerization.

http://dx.doi.org/10.5772/67576

As some polymeric materials have conductivities similar to those of metals, they represent an important research area for the next generation of organic electronic devices. Conductivities in some polymers, such as poly(3,4-ethylenedioxythiophene) (PEDOT), are comparable to those of indium oxide or tin, while showing significant optical transmission. In this work, the electrical conductivity of the thin films was evaluated by means of a four-point technique. The films' electric properties and their dependence in the presence of radiation of several wavelengths were evaluated in order to determine whether this type of PMC films may have applications in the construction of electronic and optoelectronic flexible devices, such as OLEDs, photovoltaic devices and visual information devices. Additionally, the optical activation energies were evaluated by the Cody and Tauc methods from the transmittance values of the films at different thicknesses [1, 2].

2. Research method

2.1. Crystallization process

To carry out the crystallization of MPcs embedded in a polymeric matrix, the gel crystallization method was used, where a very viscous medium that favours slow crystallization is used to mix the constituent phases, mainly by diffusion. In this method, crystal growth in the gel takes place by diffusion-controlled mass transport. This procedure minimizes the sedimentation and convection effects of traditional crystallization by evaporation methods. One must take into account that the crystallization mechanism consists of three steps, i.e. solution supersaturation, formation of crystalline nuclei and crystal growth. The gel is a means to transport molecules or ions (precipitant agents, shock absorbers), with no or almost no chemical reactivity to molecules and ions that diffuse through their three-dimensional polymeric network. Gels can be classified, according to their preparation method, as chemical or physical. Chemical gels are those obtained by poly-addition processes, like those achieved from neutralization of sodium metasilicate, or by poly-condensation processes, such as those obtained from the hydrolysis reaction of tetramethoxysilane. The physical gels, including agar and agarose, are defined as those where the gelation process is carried out by the variation of some physical parameter, like temperature.

For the current study, tetramethoxysilane gel at 10% volume, with 50% of ethanol for crystallization in FePc capillary tubes, was used. Before introducing the solved gel into the capillary, this tube must be carefully washed with detergent, followed by double-distilled water and then acetone, and finally dried with warm air. The introduction of gel into the capillary is carried out by the application of air pressure with a syringe, taking care to avoid the formation of bubbles in the gel. The gel must occupy the central 4-cm section of the capillary. After the dispersion has gelled (a process which takes about 4 weeks), MPc is added through the ends of the capillary, travelling a distance of 3 cm of length. These MPcs, previously dissolved, must be added in the same way as the gel, by means of air pressure with the help of a syringe, while taking care not to form bubbles. The capillary is then sealed at the two ends and kept at a constant temperature of 22°C, until the product is formed. The conformation of the system used for gel crystallization can be shown in **Figure 1**, where the diagram of the tube used

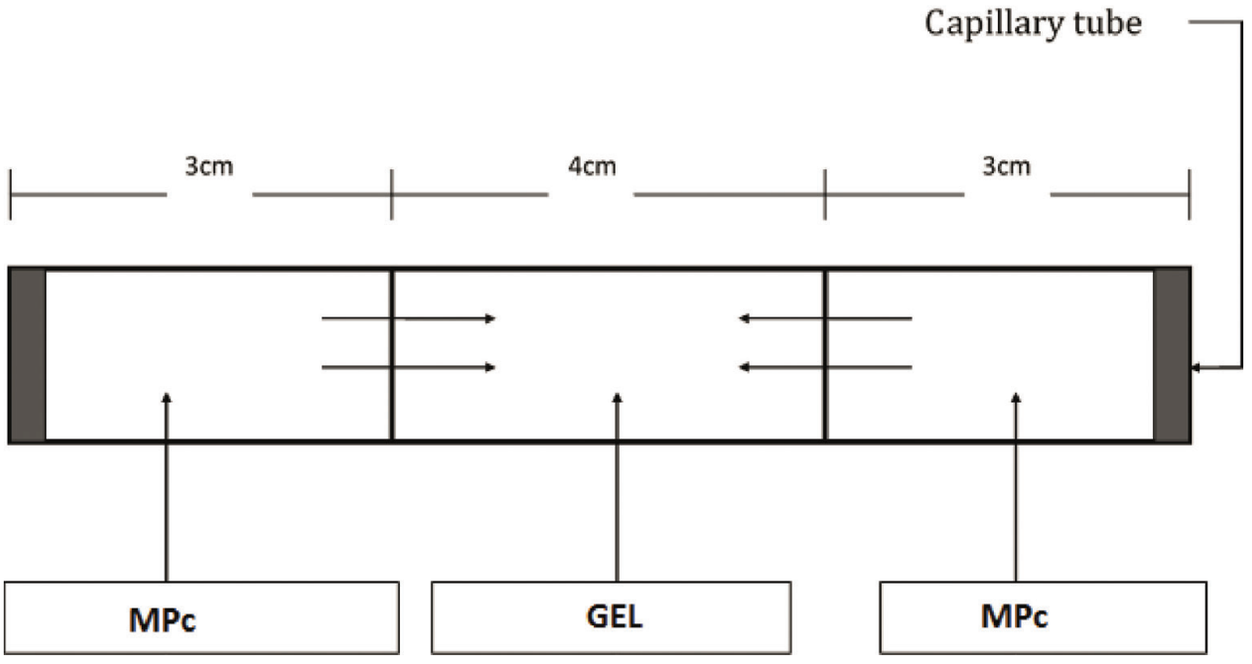

Figure 1. Capillary system used for crystallization.

for the crystallization is divided into three parts, as shown in the figure: one in the middle, where the gel was initially placed and the two ends where the dissolved MPc was placed before the MPc molecules migrated to the gel zone, where they nucleated and grew. This gel-based technique provides continuous control over the crystal or particle growth process, since it becomes possible to increase the growth rate by adding a larger amount of reagents through the ends of the capillary. Moreover, it also reduces the risk of damage to the crystal or the particle that could occur because of physical instabilities in the experimental arrangement, as it avoids the direct manipulation of the grown crystals.

2.2. Thin-film deposition and characterization

Most of the advanced devices manufactured today depend, at some point of their fabrication, on the synthesis and growth of films or thin layers. For this work, thin-film deposition of FePc particles nucleated and grown in gels was carried out in air by spin coating. The material was deposited onto a Corning 7059 glass, quartz, (100) single-crystalline silicon (c-Si) 200 Ω-cm wafers and ITO-coated glass slides. The quartz and Corning glass substrates were ultrasonically degreased in warm methanol and dried under a nitrogen atmosphere. The silicon substrates were chemically etched with a *p-etch* solution and dried under a nitrogen atmosphere. The composition of the solution was selected to have an FePc: polystyrene ratio of 1:3 in chloroform. The solution was spin coated on the substrates in a two-step process: 2500 rpm for 30 s, followed by annealing at 393 K for 10 min. These processes, spin coating and annealing, were repeated to obtain a suitable thickness. The thicknesses of the films obtained in the present study are shown in **Table 1**. We also report the determination of optical parameters related to the main transitions in the UV-Vis region, as well as the fundamental energy gap calculations for these films. Devices consisting of polystyrene matrix film were placed onto Corning

Sample	Film thickness (nm)	Direct Cody optical gap (eV)	Indirect Cody optical gap (eV)	Direct Tauc optical gap (eV)	Indirect Tauc optical gap (eV)
Thin Film 1	29	5.4	5.4	5.4	5.1
Thin Film 2	35	5.3	5.3	5.3	4.7
Thin Film 3	52	5.3	5.2	5.3	4.7
Thin Film 4	75	5.3	5.2	5.3	4.3
Thin Film 5	99	5.3	5.1	5.3	4.3
Thin Film 6	122	5.3	4.7	5.3	4.2
Thin Film 7	348	4.3	4.3	4.2	3.8

Table 1. Characteristic parameters of the FePc/polystyrene films.

glass substrates with a contact conductor of indium tin oxide (ITO) by spin coating. After the deposition, in order to diffuse MPc particles into the polystyrene matrix, the films were heat treated at 393 K for 10 min. The electric conductivity at 298 K of the device was evaluated with a four-point probe; for these measurements, the substrates were ITO-coated glasses with silver strips acting as electrodes. The strips were deposited by the painting process, the current due to hole-injection from positively-biased ITO was measured and the current due to hole-injection from silver was measured by reversing the polarity of the bias voltage [3].

2.3. Instruments

For the preparation of the thin films, a *Best Tools Smart Coater* 200, operating at 400 W, 110 V and 50/60 Hz, was used. FT-IR measurements were obtained with a Nicolet iS5-FT spectrophotometer using KBr pellets for the powders and silicon wafers as substrates for the thin films. Film thickness values were determined by profilometry in a quartz substrate with a *Bruker* profilometer, model DEKTAK XT, with STYLUS, LIS 3, 2 μm RADIUS-Type B. For SEM, a ZEISS EVO LS 10 scanning electron microscope was coupled to a microanalysis system and operated at a voltage of 20 kV and a focal distance of 25 mm, using thin films on a glass substrate. The size and distribution of dispersed particles were observed using a *JEOL* JEM2010 transmission electron microscope (TEM), LaB_6 cathode at 200 kV, 105 μA. UV-Vis spectroscopy was carried out in a *Unicam* spectrophotometer, model *UV300*, with a quartz substrate. Electric characterization was performed with a programmable voltage source, an auto-ranging pico-ammeter *Keithley* 4200-SCS-PK1 and a sensing station with a *Next Robotix* lighting controller circuit.

3. Results and discussion

The capillaries with FePc at the ends and tetramethoxysilane in the centre were allowed to stand at 22°C for 2 weeks. Subsequently, the generated particles were extracted from the capillary within the gel and were observed by SEM. **Figure 2a** and **b** show, at different magnifications, the FePc particles embedded in tetramethoxysilane. Despite being very small, they showed several structures-amorphous particles, regular particles and needles. In all cases,

there was a heterogeneous distribution of particles inside the gel. The particles were removed from the tetramethoxysilane, washed and dried in a vacuum. The use of this technique demonstrated its applicability to the *in situ* formation of nanometric-size particles inside the gel. A preliminary TEM study of the nanometric FePc particles was also performed. **Figure 2c** shows a high-resolution bright field image of the FePc sample, where particles ranging in size between 2.8 and 20 nm can be seen. The shape of the particles is irregular, although some quasi-spherical forms can be discerned. A heterogeneous dispersion of the nanoparticles can also be seen. Among the advantages of using this technique for reinforcing particles in the manufacture of composite materials are that a very small sample can be used and the continuous manipulation of particles can be avoided; furthermore, it permits a continuous control of the growth process. It is difficult to determine the crystalline arrangement from TEM imaging in real space, so a wider characterization by IR spectroscopy was required. IR spectroscopy was specifically used to identify the structural nature of FePc, given that the IR spectrum depends on the crystal structure [4]. MPcs are known to have different polymorphs which are strongly identified by the IR absorption technique [4, 5]. It has been reported that the α-form of MPc can be characterized by a band around 720 cm^{-1}, while the β-form can be characterized by a band at a greater wave number at approximately 778 cm^{-1} [4–7]. In **Table 2**, it can be observed that FePc particles were present in the α and β crystalline structures.

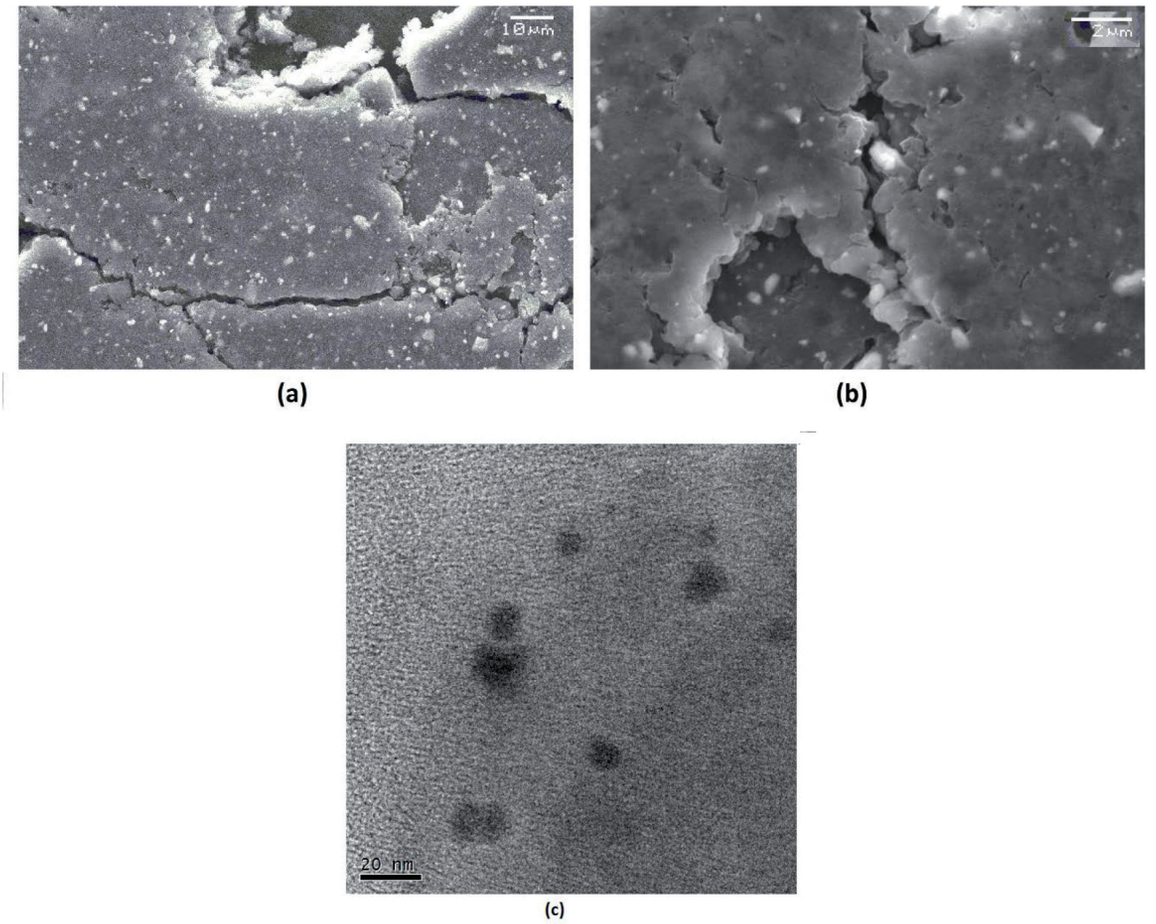

Figure 2. Gel with FePc particles (a) 1000×, (b) 7000× and (c) HRTEM micrographs.

http://dx.doi.org/10.5772/67576

Sample	ν (C—C) cm^{-1}	ν (C=N) cm^{-1}	ν (C—H) cm^{-1}	α-form cm^{-1}	β-form cm^{-1}
FePc (particle)	1609	1336	1164, 1119, 750	724	771
Thin Film 1	1607	1331	1163, 1119, 754	-	769
Thin Film 2	1609	1336	1164, 1119, 750	724	771
Thin Film 3	1603	1330	1164, 1117, 754	720	770
Thin Film 4	1604	1330	1163, 1119, 754	720	771
Thin Film 5	1604	1331	1166, 1117, 755	721	771
Thin Film 6	1603	1331	1165, 1119, 755	719	769
Thin Film 7	1603	1331	1165, 1116, 754	719	769

Table 2. Characteristic FT-IR bands for particles and thin films (cm^{-1}).

IR spectroscopy was also used in this study to ascertain the presence of the more representative bonds in the FePc compound and to determine whether significant chemical changes took place in this compound during gel nucleation and growth. **Table 2** shows the characteristic bands of the FePc particles deposited in the gel. The band appearing at 1605 ± 4 cm^{-1} was assigned to the C=C stretching vibration for pyrrole. The peak responsible for carbon-nitrogen stretching and bending occurs at 1332 ± 4 cm^{-1}. The peaks located at 1164 ± 2, 1117 ± 2 and 753 ± 2 cm^{-1} are due to the interaction of carbon atoms with the peripheral-ring hydrogen atoms [8–10]. As mentioned above, spin coating and annealing were carried out to produce the thin films. IR spectroscopy was performed in these films in order to verify that no chemical changes occurred in the FePc when interacting with the polymeric matrix. The results reported in **Table 2** indicate that the MPc did not experience any chemical changes during the deposition; on the other hand, in the thinnest film, the crystalline phase α is not observed. It is worth mentioning that the signals in the MPc film show slight changes in location. This occurs because, in thin films deposited by any method, internal stress affects intramolecular angles and bonding energies. Nevertheless, no significant changes occurred in these films, so we may conclude that the production of thin films from the FePc-polystyrene composite by the spin coating and annealing method is appropriate.

The films obtained by spin-coating were analysed by SEM. **Figure 3** shows the presence of the two phases-polymeric matrix and reinforcement. During the annealing, polymerization of polystyrene generated the needles shown in the images, while the FePc appears as irregular conglomerates. It is possible to observe that the MPc particles have been embedded in the matrix homogeneously, i.e. the particles are not agglomerated or separated, which in turn indicates that polystyrene is an appropriate matrix for this kind of films.

Optical absorption measurements are widely used to characterize the electronic properties of the thin films through the determination of parameters describing the electronic transitions, such as the band gap [11]. Additionally, the absorption spectra of different polymorphs of some Pc compounds show significant differences among each other [7, 12]. MPcs have two typical absorption bands, namely the *Q*-band in the visible region and the *B* or Soret-band in the near-ultraviolet

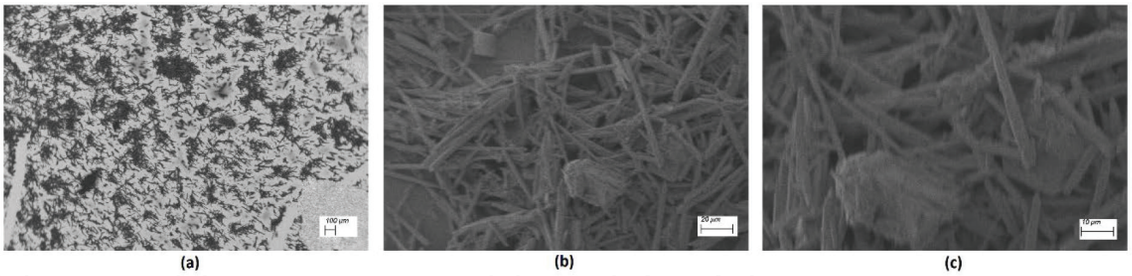

Figure 3. SEM images for spin-coated films (a) 83×, (b) 500× y (c) 1000×.

region [13–17]. The Q-band absorption is responsible for the characteristically intense blue/green colour of the FePc and this band has been interpreted in terms of π-π* excitation between bonding and antibonding molecular orbitals [7, 18]. The electronic spectrum of the FePc particles obtained in tetramethoxysilane (**Figure 4a**) shows the characteristic Q-band absorption in the 578–750 nm region. The Soret-band of FePc arising from the deeper π levels → LUMO transitions is observed in the UV region at about 400–463 nm. On the other hand, the optical transmittance spectra of the thin-films deposited on quartz were recorded from 200 to 1100 nm and are shown in **Figure 4b**. Differences in the transmittance of the films under examination can be attributed to differences in thickness (see **Table 1**) according to Beer's law [19]. When the thickness of the film increases, its transmittance diminishes. The UV-Vis spectra of FePc-polystyrene thin films exhibited a characteristic B-band in the region between 285 and 305 nm. The observation of a single peak in the Soret band resembles that observed for CoPc, NiPc and other Pc thin films [20, 21]. This may imply that the splitting structure of this peak could be affected by the orbital overlap of the Pc ring with the central metal [21], although this effect could also be attributed to the presence of the polymeric matrix which, while protecting the FePc from oxygen and environmental humidity, also alters its optical properties in the visible region of the spectrum.

Considering the above results, we further apply the Cody and the Tauc models for the determination of the band gaps of the thin films [7, 22, 23]. The Cody model provides an effective option for the determination of the optical band of thin films in terms of its thickness. It uses the dependence between the photon energy ($h\nu$) and the absorption coefficient (α). The optical gap associated with the thin films is determined by extrapolating the linear trend observed in the spectral dependence of $(\alpha/h\nu)^n$ on $h\nu$. Here, n is a number characterizing the transition process, depending upon the nature of the electronic transitions responsible for the absorption; for direct transitions, $n = ½$, and, for indirect transitions, $n = 2$. The intersection with the x-axis of this linear extrapolation corresponds to the Cody optical gap for a given thickness of the film [22, 23]. The Cody optical gaps Eg_i and Eg_d for both transitions were obtained from the curves corresponding to those shown in **Figure 5** for the film with the largest thickness (*Thin Film 7*), which was of 348 nm.

For this film, the optical gap value is similar for both transitions, direct and indirect (see **Table 1**); apparently, the high concentration of FePc related to the highest thickness could be the cause of the similar values, but this could also be related to the fact that 4.3 eV is the lower (indirect) gap of the films under examination and may be quantitatively close to the direct gap for that particular film. On the other hand, the Tauc model argues that the optical gap associated with the thin film is determined through an extrapolation of the linear trend observed in the spectral

http://dx.doi.org/10.5772/67576

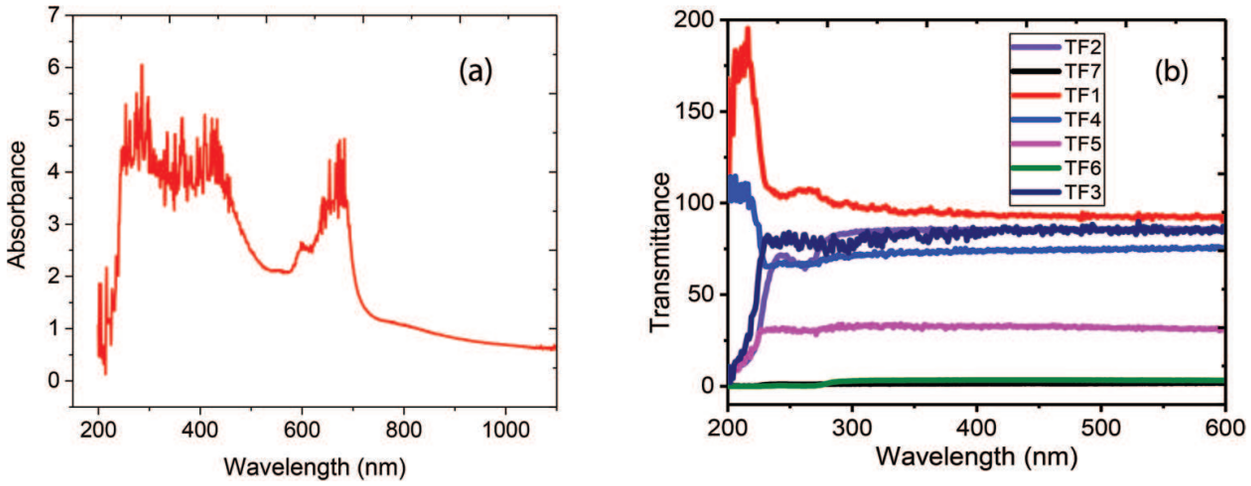

Figure 4. UV-Vis spectroscopy for: (a) FePc and (b) thin films.

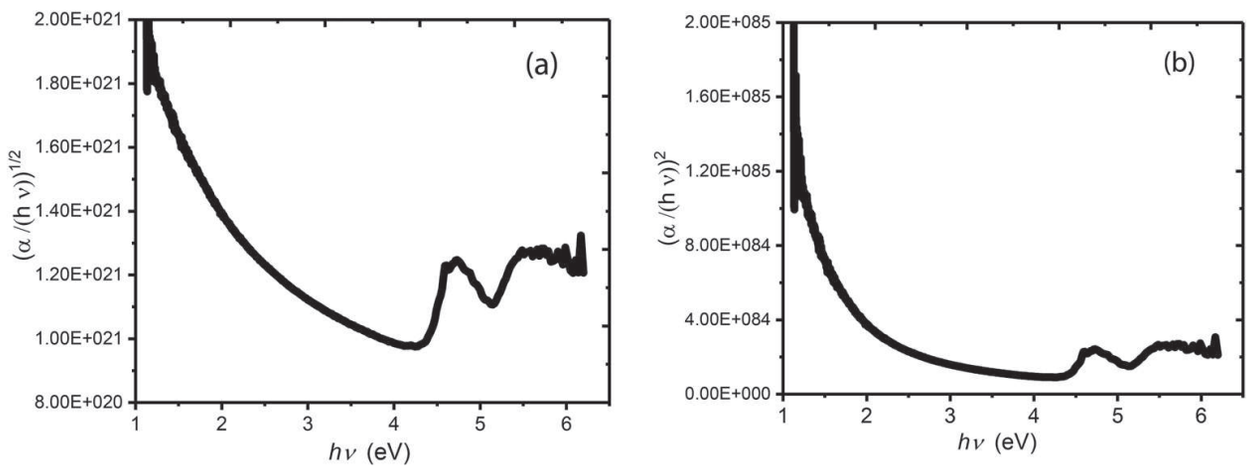

Figure 5. Plot of (a) $(\alpha/h\nu)^{1/2}$ and (b) $(\alpha/h\nu)^2$ versus photon energy $h\nu$ of *Thin Film 7*.

dependence of $(\alpha h\nu)^n$ over a limited range of $h\nu$ [1, 2]. The Tauc optical gaps for Eg_i and Eg_d were obtained from the curves corresponding (see **Table 1**) and they are shown in **Figure 6** for the film with the largest thickness (*Thin Film 7*). According to **Table 1** for the thicker film the smaller gap is obtained. At this thickness, the concentration of FePc is sufficient to decrease the gap and increase the overlap between Pc molecules. As the stacking between molecules increases, the electron flux increases significantly with respect to films with small thickness. On the other hand, for each of the remaining films, the indirect transition is the predominant one, with significantly lower values than the direct transition; this may be expected because of the mainly amorphous characteristics of the films and their effect on orbital overlap, despite FePc showing some α or β crystalline forms. It is important to mention that the variations in optical gaps obtained for the different films are of low significance. This may be attributed to the similar morphology of these systems, which differ only in the quantity and size of the FePc particles and the arrangement of their molecules in the polymeric matrix. Additionally, the gap depends on the number of electrons of the metal in the Pc ring [7, 19], which is the same for all these films.

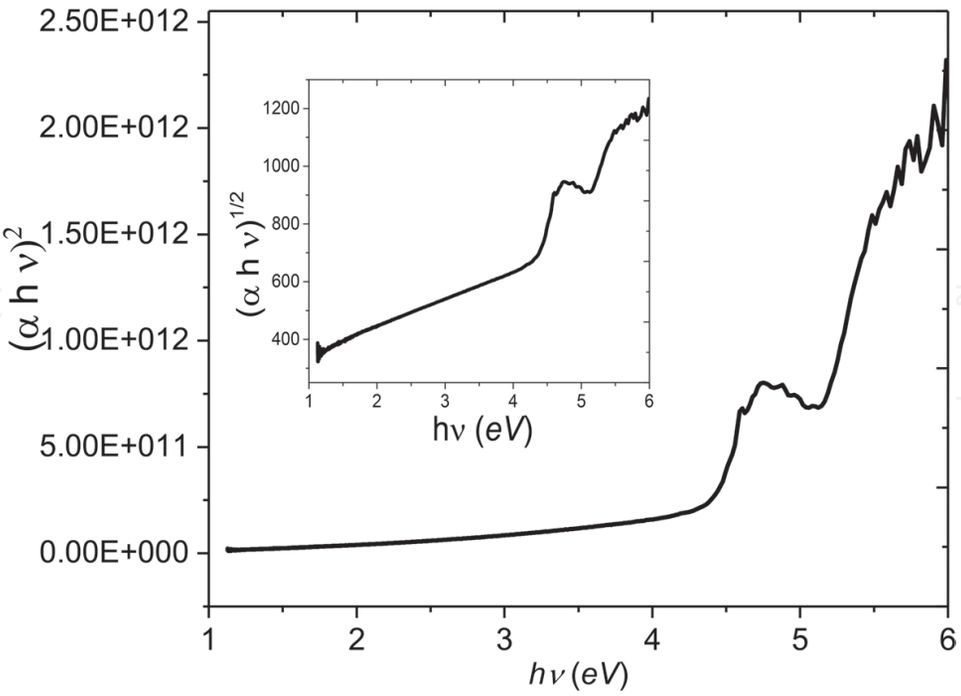

Figure 6. Plot of $(\alpha h\nu)^{1/2}$ and $(\alpha h\nu)^2$ versus photon energy $h\nu$ of *Thin Film 7*.

Finally, in order to evaluate the electrical properties of the thin films, the four-point technique was employed, using the glass substrate with an ITO conducting contact. This study was performed on the sample labelled *Thin Film 7*, which was the one having the lowest optical gap. The film had a surface area of 2.16 cm^2. **Figure 7** shows the *I-V* characteristics of *Thin Film 7* under different illumination types (yellow light, white, blue, orange, green, infrared, UV and dark [no light]). Regardless of the wavelength of the incident radiation, the thin film follows the same behaviour. At lower voltages (around 10 V), ohmic conduction is evident, while space-charge limited conductivity (SCLC) governed by an exponential trap distribution is found at higher voltages. On the other hand, the *I-V* characteristics display symmetric

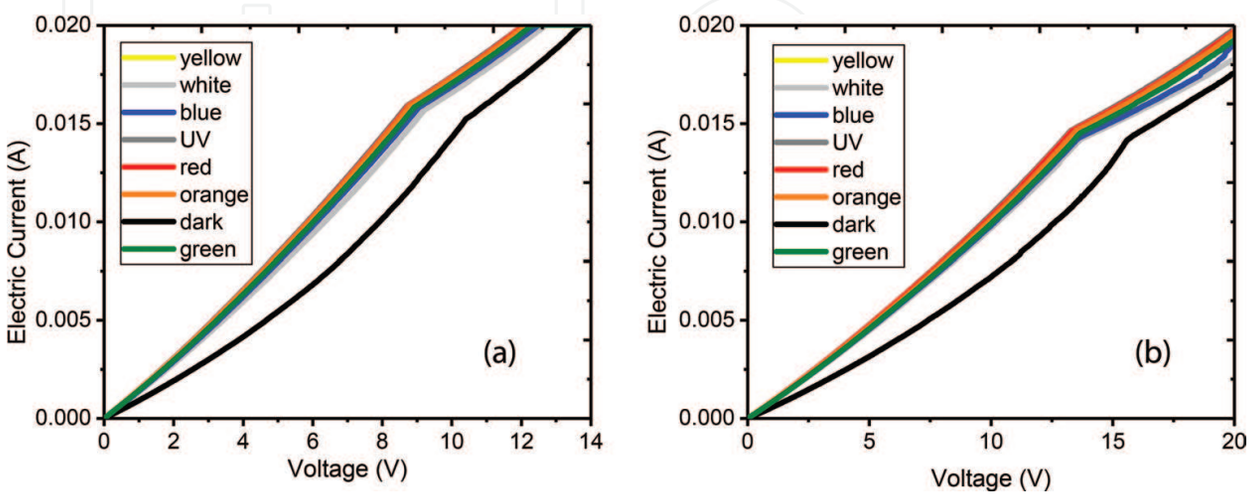

Figure 7. *I-V* characteristics of *Thin Film 7:* (a) ITO is positively biased and (b) ITO is negatively biased.

http://dx.doi.org/10.5772/67576

behaviour, both when (a) the current due to hole injection from positively biased ITO was measured and also when (b) the current due to hole injection from silver was measured by reversing the polarity of the bias voltage. This can be explained by a negligible energy barrier at the *ITO/FePc-polystyrene* and *FePc-polystyrene/Ag* interfaces leading to a SCL bulk current when either the ITO or silver electrode is positively biased [24–26].

4. Conclusions

Different types of particles and crystalline polymorphs of FePc can be obtained with tetramethoxysilane. This blend of structures can be used to produce thin films of a polystyrene matrix in a FePc matrix-reinforcing base by spin coating. Upon examination of the resulting films by SEM, a homogeneous particle distribution is found within the polystyrene matrix. IR spectral analysis confirms that FePc is rich in α and β polymorphs. None of the MPc samples suffers chemical degradation during the thin-film deposition and annealing processes. The UV-Vis spectra of the particles in tetramethoxysilane show two well-defined absorption bands, namely, the Soret and the Q-bands. The exact position of these bands depends on their particular structure, metal complexation, and peripheral substituents. However, only the Soret band appears in the UV-Vis spectra of the thin films, which can be attributed to the presence of the polymeric matrix. The optical gap was calculated from the Cody and Tauc models and the information obtained from the absorption spectra indicates that these films absorb light on either side of the blue-green region. Since these FePc compounds absorb light on either side of the blue-green spectrum, they could be used as photosensitive materials in practical applications. The electrical conductivity of the films was evaluated and ohmic characteristics were found at low voltages, while an SCLC-type behaviour can be observed at higher voltages. Bias inversion in the *I-V* measurements does not have a significant effect on the thin-film electric transport characteristics.

Acknowledgements

The authors wish to thank the technical support of M.I. Mariel Leyva-Esqueda (Universidad Anáhuac) for technical help. María Elena Sánchez-Vergara gratefully acknowledges the financial support of Universidad Anáhuac México under grant INNADBSEVM140129141.

Author details

María Elena Sánchez-Vergara[1]*, Angelina Romo Ubeda[1], Enrique Garibay Ochoa[2] and José Ramón Alvarez-Bada[1]

*Address all correspondence to: elena.sanchez@anahuac.mx

1 School of Engineering, The Anahuac University Mexico, State of Mexico, Mexico

2 Technological Institute of Morelia, José María Morelos y Pavón, Morelia, Michoacán, Mexico

References

[1] Mok T.M., O'Leary S.K. The dependence of the Tauc and Cody optical gaps associated with hydrogenated amorphous silicon on the film thickness: *αl* experimental limitations and the impact of curvature in the Tauc and Cody plots. Journal of Applied Physics. 2007;102:113525. DOI: 10.1063/1.2817822.

[2] O'Leary S. K., Lim P. K. On determining the optical gap associated with an amorphous semiconductor: a generalization of the Tauc model. Solid State Communications. 1997;104(1):17–21. DOI: 10.1016/s0038-1098(97)00268-8.

[3] Mahapatro A.K., Ghosh S. Charge carrier transport in metal phthalocyanine based disordered thin films. Journal of Applied Physics. 2007;101:034318-1–034318-5. DOI: 10.1063/1.2434946.

[4] Karan S., Basak D., Mallik B. Persistence in photoconductivity and optical property of nanostructured copper (II) phthalocyanine thin films. Current Applied Physics. 2010;10(4):1117–1122. DOI: 10.1016/j.cap.2010.01.011.

[5] Wang J.B., Li W.L., Chu B., Lee C.S., Su Z.S., Zhang G., Wu S.H., Yan F. High speed responsive near infrared photodetector focusing on 808 nm radiation using hexadecafluoro–copper–phthalocyanine as the acceptor. Organic Electronics. 2011;12(1):34–38. DOI: 10.1016/j.orgel.2010.09.015.

[6] Neghabi M., Zadsar M., Ghorashi S.M.B. Investigation of structural and optoelectronic properties of annealed nickel phthalocyanine thin films. Materials Science in Semiconductor Processing. 2014;17:13–20. DOI: 10.1016/j.mssp.2013.08.002.

[7] El-Nahass M.M., Farag, A.M., Abd El-Rahman K.F., Darwish A.A.A. Dispersion studies and electronic transitions in nickel phthalocyanine thin films. Optics & Laser Technology 2005;37(7):513–523. DOI: 10.1016/j.optlastec.2004.08.016.

[8] Berhanu S., Tariq F., Jones T., McComb D.W. Three-dimensionally interconnected organic nanocomposite thin films: implications for donor–acceptor photovoltaic applications. Journal of Materials Chemistry. 2010;20(37):8005–8009. DOI: 10.1039/c0jm01030h.

[9] Farag A.A.M., Yahia I.S., Alfaify S., Bilgiçli A., Kandaz M., Yakuphanoğlu F. Optical dispersion parameters based on single-oscillator model and optical absorption of nanocrystalline metal phthalocyanine films: a comparison study. Superlattices and Microstructures. 2013;60:83–100. DOI: 10.1016/j.spmi.2013.04.018.

[10] Liu L.Y., Wan L., Cao L., Han Y.Y., Zhang W.H., Chen T.X., Guo P.P., Wang K., Xu F.Q. Assistance of partially reduced MoO_3 interlayer to hole-injection at iron phthalocyanine/ITO interface evidenced by photoemission study. Applied Surface Science. 2013;271:352–356. DOI: 10.1016/j.apsusc.2013.01.200.

[11] Yang Y., Samas B., Kennedy V.O., Macikenas D., Chaloux B.L., Miller J.A., Speer R.L., Protasiewicz J., Pinkerton A.A., Kenney M.E. Long, directional interactions in cofacial

silicon phthalocyanine oligomers. The Journal of Physical Chemistry A. 2011;115(45):12474–12485. DOI: 10.1021/jp2019445.

[12] Lbova A.K., Vasiliev M.P., Gutmann E.S. Phthalocyanine and polystyrene film nanocomposites. Russian Journal of Physical Chemistry A. 2011;85(3):457–561. DOI: 10.1134/S0036024411030216.

[13] Liu Z.T., Kwok H.S., Djurišić A.B. The optical functions of metal phthalocyanines. Journal of Physics D: Applied Physics. 2004;37(5):678–688. DOI: 10.1088/0022-3727/37/5/006.

[14] Ottaviano L., Di Nardo S., Lozzi L., Passacantando M., Picozzi P., Santucci S. Thin and ultra-thin films of nickel phthalocyanine grown on highly oriented pyrolitic graphite: an XPS, UHV-AFM and air tapping-mode AFM study. Surface Science. 1997;373(2–3):318–332. DOI: 10.1016/s0039-6028(96)01179.

[15] Guo L., Ma G., Liu Y., Mi J., Qian S., Qiu L. Optical and non-linear optical properties of vanadium oxide phthalocyanine films. Applied Physics B. 2014;74(3):253–257. DOI: 10.1007/s003400200801.

[16] Djurišić A.B., Kwong C.Y., Lau T.W., Guo W.L., Li E.H., Liu Z.T., Kwok H.S., Lam L.S.M., Chan W.K. Optical properties of copper phthalocyanine. Optics Communications. 2002;205(1–3):155–162. DOI: 10.1016/s0030-4018(02)01311-1.

[17] Andzelm J., Rawlett A.M., Orlicki J.A., Snyder J.F., Baldridge K.K. Optical properties of phthalocyanine and naphthalocyanine compounds. Journal of Chemical Theory and Computation. 2007;3(3):870–877. DOI: 10.1021/ct700017b.

[18] Nitschke C., O'Flaherty S.M., Kroell M., Strevens A., Maier S., Rüther M.G., Blau W.J. Preparation and nonlinear optical properties of phthalocyanine nanocrystals. In: Organic Photonic Materials and Devices; 25 January 2003; San Jose, CA. James V., Grote G., Kaino T., Editors, Proceedings of SPIE. 2003, Vol. 4991, pp. 124–131.

[19] Seoudi R., El-Bahy G.S., El Sayed Z.A. Ultraviolet and visible spectroscopic studies of phthalocyanine and its complexes thin films. Optical Materials. 2006;29(2–3):304–312. DOI: 10.1016/j.optmat.2005.10.002.

[20] El-Nahass M.M., Sallam M.M.A. Optical properties of thermally evaporated metal-free phthalocyanine (h 2 pc) thin films. International Journal of Modern Physics B. 2005;19(27):4057–4071. DOI: 10.1142/s0217979205032632.

[21] El-Nahass M.M., Abd-El-Rahman K.F., Darwish A.A.A. Fourier-transform infrared and UV-Vis spectroscopes of nickel phthalocyanine thin films. Materials Chemistry and Physics. 2005;92(1):185–189. DOI: 10.1016/j.matchemphys.2005.01.008.

[22] Cody G., Tiedje T., Abeles B., Brooks B., Goldstein Y. Disorder and the optical-absorption edge of hydrogenated amorphous silicon. Physical Review Letters. 1981;47(20):1480–1483. DOI: 10.1103/physrevlett.47.1480.

[23] Cody G.D. Chapter 2 The Optical Absorption Edge of a-Si:H. Hydrogenated Amorphous Silicon-Optical Properties. Semiconductors and Semimetals. 1984;21(Part B):11–82. DOI: 10.1016/s0080-8784(08)62910-5.

[24] Anthopoulos T.D., Shafai T.S. SCLC measurements in nickel phthalocyanine thin films. Physica Status Solidi (A). 2000;181(2):569–574. DOI: 10.1002/1521-396X (200010).

[25] Gravano S., Hassan A.K., Gould R.D. Effects of annealing on the trap distribution of cobalt phthalocyanine thin films. International Journal of Electronics. 1991;70(3):477–484. DOI:10.1080/00207219108921297.

[26] Hassan A.K., Gould R.D. The interpretation of current density-voltage and activation energy measurements on freshly prepared and heat treated nickel phthalocyanine thin films. International Journal of Electronics. 1993;74(1):59–65. DOI:10.1080/00207219308925813.

IntechOpen